Int. J. Heat Mass Transfer. Vol. 27, No. 8, pp. 1311–1318, 1984
Printed in Great Britain

0017–9310/84 $3.00 + 0.00
Pergamon Press Ltd.

TRANSIENT BOILING HEAT TRANSFER FROM TWO DIFFERENT HEAT SOURCES: SMALL DIAMETER WIRE AND THIN FILM FLAT SURFACE ON A QUARTZ SUBSTRATE

PATRICIA J. GIARRATANO
Chemical Engineering Science Division, Center for Chemical Engineering, National Bureau of Standards, Boulder, CO 80303, U.S.A.

(*Received* 18 *March* 1983 *and in revised form* 31 *October* 1983)

Abstract—Transient boiling heat transfer data are reported for two different heater surface geometries submerged in liquid nitrogen. During the early part of the transient heat pulse, the heat transfer coefficient for both geometries generally agrees with values predicted from classical transient pure conduction equations. The agreement persists until the time for onset of convection which varies approximately as $1/q^2$ where q is the heat flux to the fluid.

INTRODUCTION

HEAT transfer rates during processes where heat flux and/or surface temperature and/or fluid velocities change rapidly in time are not generally predictable from correlations developed from steady-state measurements [1–4]. Differences often are due to compressible fluid effects, or vapor nucleation phenomena.

Study of dynamic processes can be by:

(1) time-resolved measurements of heat flux and surface temperature rise ($q, \Delta T$), i.e. standard procedure but adding time as a variable; or

(2) measurement of dynamics within the fluid using, for example, optical techniques.

The Center for Chemical Engineering of the National Bureau of Standards at Boulder, Colorado, has started a research project to study heat transfer in dynamic processes involving both processes (1) and (2) above, but this paper deals with process (1) using two heater/thermometers of two different geometries (a thin platinum film flat surface and a small diameter platinum wire).

This paper may be considered an extension of the work reported in refs. [1–3] where the heater/thermometer was a thin carbon film supported by a quartz substrate and data were for liquid or supercritical helium. For the current work platinum was selected as the heater/thermometer material because of its more suitable temperature coefficient of resistance at elevated temperatures. Also the metallic surface (platinum) is more representative of that found in various engineering applications.

The data reported in this paper were gathered while investigating the suitability of different heaters for use in our optical facility which will be used for more extensive transient heat and mass transfer measurements within the fluid. The similarities and differences in results observed for the two geometries are reported herein.

The flat geometry was selected to avoid size effects which may be evident with small diameter wires having dimensions of the order of the boundary layer thickness or bubble sizes. However, because the very thin platinum film used in the flat surface requires a supporting medium (quartz, in our system), it has the experimental disadvantage of requiring an accounting for the instantaneous heat flow into the substrate. This has been taken into account. However, for fluid media where the heat transfer is poor, the correction is large compared with the heat flow to the surrounding fluid. This can result in large experimental errors in the fluid heat flow determination. (In our original transient heat transfer studies at liquid helium temperatures, the correction for the substrate heat flow was negligible because of small heat capacity of solids at 4 K.)

The small diameter platinum wire was therefore included as an alternative heat transfer surface and thermometer because the correction to the heat flux measurement is substantially smaller and mathematically simpler. The corrections for both geometries are discussed in the following text.

The fluid for the data presented is liquid nitrogen vented to atmospheric pressure (approximately 0.83×10^5 Pa) at Boulder, Colorado.

EXPERIMENTAL APPARATUS

Two heater surface geometries were used in the experiments. Both heaters served also as thermometers for determining the solid–fluid interface temperature.

One geometry was a 35 mm $\times$ 8 mm $\times$ 35 nm platinum film which had been vapor-deposited on a 0.15875 cm fused quartz substrate. A second platinum film was located on the back side of the quartz substrate. The film on the back side of the substrate served only as a thermometer and the data from that thermometer were applied in the substrate heat flow correction discussed later in the text. The construction, calibration, and performance details of the platinum films have been previously reported [5]. Figure 1 shows the platinum film and quartz substrate assembled in the fiber-filled phenolic plastic holder.

The second geometry was a 25.4 μm diameter, 7 cm long platinum wire. Samples of the wire taken from the

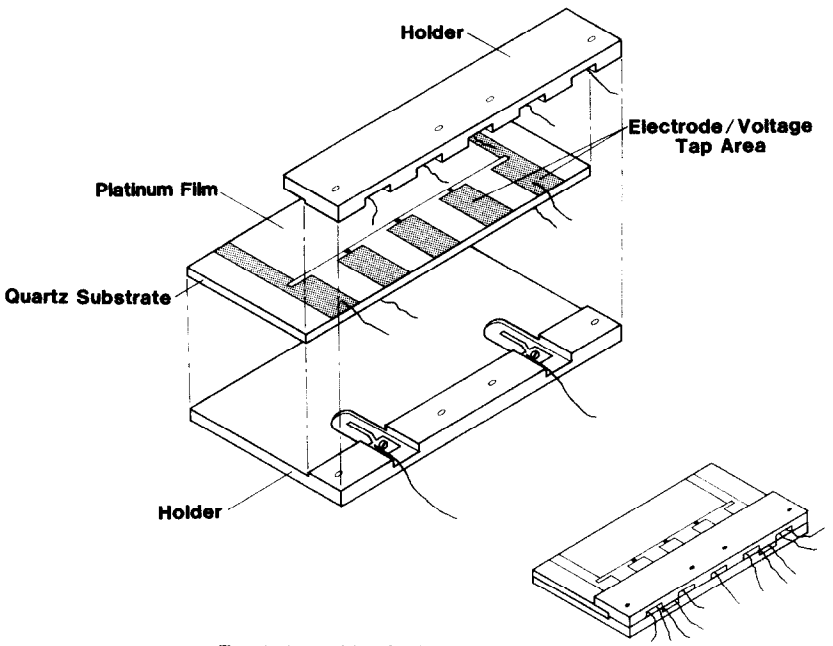

FIG. 1. Assembly of substrate and holder.

same spool as the test sample had been calibrated previously by Roder [6]. That calibration data were applied in the data reduction program with slight correction factors as dictated by *in situ* measurements at room temperature, liquid nitrogen temperature, and boiling water temperature.

The wire was soldered between and supported by two twisted thin copper sheet brackets which were mounted on a fiber-filled phenolic plastic holder. A schematic of the assembly is shown in Fig. 2.

Either test sample (wire or thin film) could be mounted on a probe which was inserted in a liquid nitrogen containment vessel vented to atmospheric pressure.

The wire was oriented horizontally and the thin platinum film was oriented with the 35 mm dimension vertical.

TEST PROCEDURE

For both test samples, a voltage pulse of variable duration was applied to the electrical circuit containing the test sample load in series with a 10 Ω standard resistor. The resulting current was essentially constant through the platinum wire test sample when the temperature was near 76 K since the wire resistance was small (approximately 2.5 Ω) compared to the 10 Ω standard resistor. This resulted in an increase in joule heating as the resistance (temperature) of the wire increased during the pulse. The magnitude of the increase depended on the magnitude of the applied voltage pulse. At the higher temperatures for the wire and for all temperatures for the flat surface (thin platinum film) the current (and joule heating) decreased with time during the pulse since the sample resistance was of the same order or larger than the 10 Ω standard resistor. The voltage drop across the test sample and across the standard resistor were fed into a digital recording oscilloscope. Subsequently, the data were transferred to a minicomputer where the recorded voltages were transformed to temperature and applied heat flux as a function of time.

The voltage pulse duration ranged from 1 ms to as long as 10 s for low level voltages. The limitation was the temperature rise of the test sample in order to stay below a 'burnout' level of temperature.

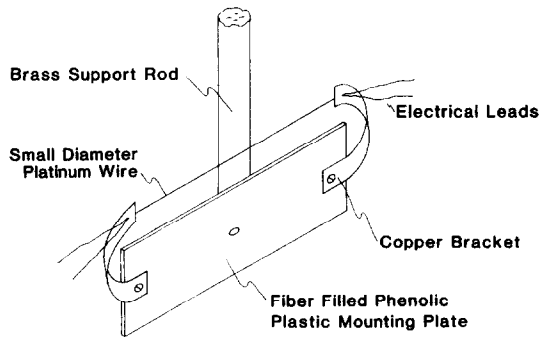

FIG. 2. Assembly of small diameter wire and support pieces.

DATA REDUCTION

As mentioned in the introduction a correction to the applied power or heat flux was required to account for the heat flow into the substrate (in the case of the flat surface) and to account for the heat capacity and mass of the wire (in the case of the platinum wire test sample).

For the wire one has

$$q_{\text{fluid}} = q_{\text{applied}} - \rho \frac{D}{4} C_p(T) \frac{dT}{dt}, \qquad (1)$$

where q_{fluid} is the heat flux to the fluid [W cm^{-2}], $q_{applied}$ is the total applied heat flux [W cm^{-2}], ρ is the density of platinum [g cm^{-3}], C_p is the heat capacity of platinum [J g^{-1} K^{-1}], dT/dt is the derivative of temperature with respect to time [K s^{-1}], and D is the diameter of the wire [cm].

The density, ρ, and the capacity as a function of temperature, $C_p(T)$, were taken from refs. [7, 8], respectively. The value dT/dt was obtained from the experimental data and, because of the small wire size, radial variation of temperature and heat loss from the ends were neglected.

For the thin film on the quartz substrate

$$\frac{\partial T}{\partial t} = \alpha \frac{\partial^2 T}{\partial X^2}, \tag{2}$$

where T is the temperature [K], α is the thermal diffusivity of quartz [cm^2 s^{-1}], X is the spatial coordinate in the substrate, normal to the heater surface [cm], and t is the time [s] subject to boundary conditions

$$t > 0 \begin{cases} X = 0, \quad T = T_{top}(t) \\ \quad \text{(measured with heater surface/thermometer)}, \\ X = 0.15875\,\text{cm}, \quad T = T_{bottom}(t) \\ \quad \text{(measured with back side thermometer)}, \end{cases}$$

$$X \geqslant 0, \quad t = 0, \quad T = T_{fluid}^{bulk} = T_0.$$

Equation (2) and the accompanying boundary conditions were solved for each run. A digital computer package [9] was used to obtain the numerical solution which provided the instantaneous temperature distribution in the quartz substrate. This yields the instantaneous heat flux into the quartz substrate, i.e.

$$q_{substrate}(t) = -k(T)\left.\frac{dT}{dX}\right|_{X=0}, \tag{3}$$

where $k(T)$ is the thermal conductivity of the quartz substrate [W cm^{-1} K^{-1}]. Published values of the thermal conductivity of quartz were used in this calculation [10]. Using a transient procedure, the thermal conductivity of the quartz substrate was measured at a few convenient temperatures [5] to support the use of published thermal conductivity values.

Finally

$$q_{fluid} = q_{applied} - q_{substrate}. \tag{4}$$

An expression for the ratio of the heat flow to the fluid to the heat flow to the substrate during *pure conduction* heat transfer, i.e. before any convection or boiling are established in the fluid, is (14), p. 71

$$\frac{q_{fluid}}{q_{substrate}} = \frac{(k/\sqrt{\alpha})_{fluid}}{(k/\sqrt{\alpha})_{substrate}}. \tag{5}$$

For most liquids and quartz substrate, this ratio is approximately 0.5, however, for most gases at room temperature, even at high pressure, this ratio is 10^{-1} or less. Thus, the thin platinum films are not suitable for gaseous data because of the large uncertainties in the heat flux to the fluid calculation [equations (3) and (4)].

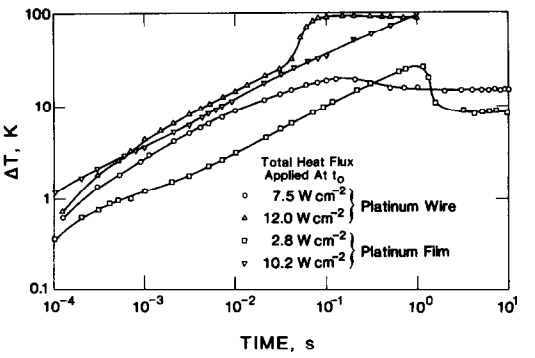

FIG. 3. Example of surface temperature rise during a step in heat flux.

Note again that equation (5) is for pure conduction only, and for enhanced heat transfer mechanisms that may occur subsequently during the heat pulse (such as nucleate boiling) the magnitude of the substrate correction is reduced. Equation (5) puts an upper bound on the magnitude of the correction.

RESULTS AND DISCUSSION

Examples of surface temperature rise during a step in heat flux are shown in Fig. 3. The experimental transient heat transfer coefficients, h, for both geometries are shown in Figs. 4 and 5. Also shown in Figs. 4 and 5 are the theoretical pure conduction transient heat transfer coefficients based on liquid and vapor properties. The theoretical equations applied were those according to Carslaw and Jaeger [11, pp. 221 and 56].

For the wire geometry

$$\Delta T = -\frac{q_0'}{4\pi k} Ei\left(\frac{-r^2}{4\alpha t}\right). \tag{6}$$

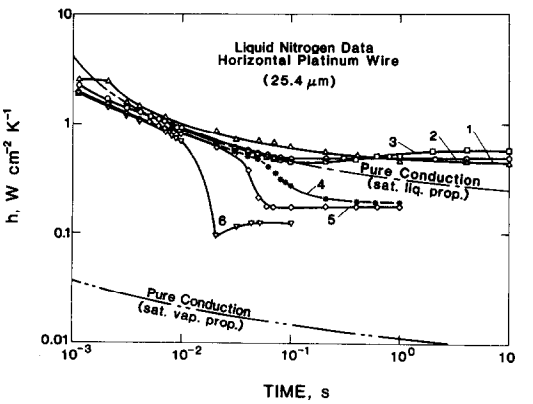

FIG. 4. Transient heat transfer coefficients for small diameter platinum wire heater surface submerged in liquid nitrogen. Total heat flux applied at t_0: 0.8 W cm^{-2} (Curve 1); 5 W cm^{-2} (Curve 2); 7.5 W cm^{-2} (Curve 3); 10 W cm^{-2} (Curve 4); 12 W cm^{-2} (Curve 5); 18 W cm^{-2} (Curve 6).

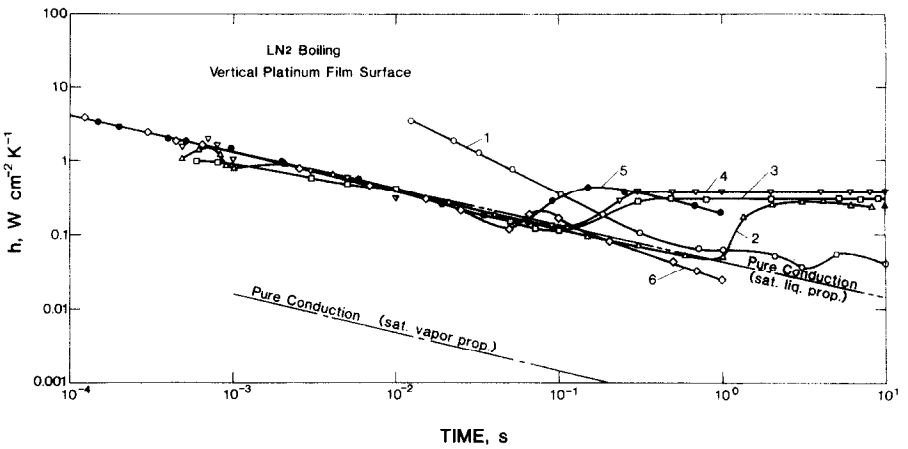

FIG. 5. Transient heat transfer coefficients for vertical thin platinum film heat surface submerged in liquid nitrogen. Total heat flux applied at t_0: 1.68 W cm^{-2} (Curve 1); 2.8 W cm^{-2} (Curve 2); 4.2 W cm^{-2} (Curve 3); 5.3 W cm^{-2} (Curve 4); 9.2 W cm^{-2} (Curve 5); 10.2 W cm^{-2} (Curve 6).

For the thin film geometry

$$\Delta T = \frac{2q_0}{k}\left(\frac{\alpha t}{\pi}\right)^{1/2}, \tag{7}$$

where ΔT is the surface temperature rise, $T_{surf} - T_{bulk}$ [K], q_0' is the heat to fluid per unit length [W cm^{-1}], q_0 is the heat flux to fluid [W cm^{-2}], k is the thermal conductivity [W cm^{-1} K^{-1}], α is the thermal diffusivity [cm^2 s^{-1}], r is the radius of wire [cm], and t is the time [s]. The typical behavior of the curves shown in the figures has been observed and reported by other investigators [1, 12–14]. Oker and Merte's [12] high-speed films of the transient boiling process provide a description which can be related to the experimental transient heat transfer coefficients shown in Figs. 4 and 5. For heat fluxes below the critical heat flux, at the beginning of the transient, heat is transferred by pure conduction from the heating surface to the fluid. This can be seen by the fairly good agreement at short times between the experimental heat transfer coefficient and the theoretical h_{cond} shown in Figs. 4 and 5. Subsequent to the pure conduction period, natural convection commences but persists for a relatively short time before nucleate boiling spreads over the surface. These two regimes of heat transfer are evident from the deviation of our low heat flux data upward from the pure conduction curve for liquid in Figs. 4 and 5 and by the decrease in temperature following an initial increase shown in Fig. 3 for the low heat flux data. In this investigation there was no visual way of distinguishing natural convection from the initiation of boiling. For heat fluxes above the critical, the early part of the transient is again represented by pure conduction, but then the deviation of the high heat flux experimental data is generally downward from the liquid pure conduction curve, signaling a transition to film boiling. While not seen in Fig. 4 for the wire geometry, the thin film results in Fig. 5 show there was an apparent short-term increase in h before the decrease to film boiling as shown by Curves 5 and 6. This short-term increase in h may be representative of a metastable nucleation period before the transition to film boiling as noted by Steward [1]. Finally, note that the film boiling coefficient lies between the liquid h_{cond} and the vapor h_{cond}. This is reasonable since the theoretical calculations for pure conduction were based on a model of a semi-infinite medium heated at the surface (for the flat surface geometry) and a continuous line source surrounded by an infinite medium (for the wire geometry). The calculation for a finite vapor film with liquid above it (as is the case for film boiling) would be expected to be somewhere between these two cases.

Oker and Merte [12] correlated the time to the onset of natural convection (time at which h_{exp} begins to deviate from h_{cond}) with the heat flux to the fluid. Such a correlation is shown in Fig. 6 and includes the data of this study as well as other investigators. For our data τ was taken to be that corresponding to the time when the

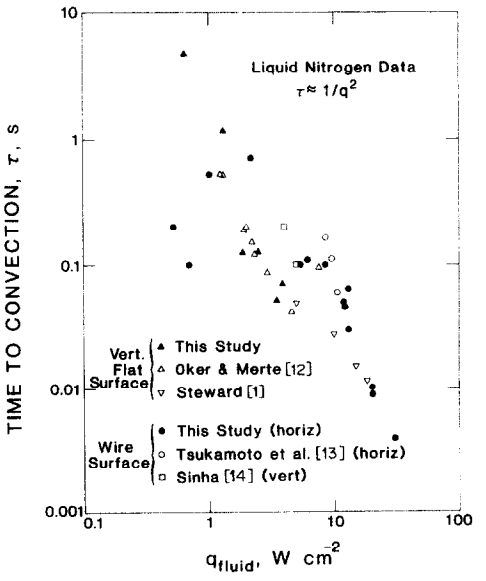

FIG. 6. Time to onset of convection vs heat flux to the fluid.

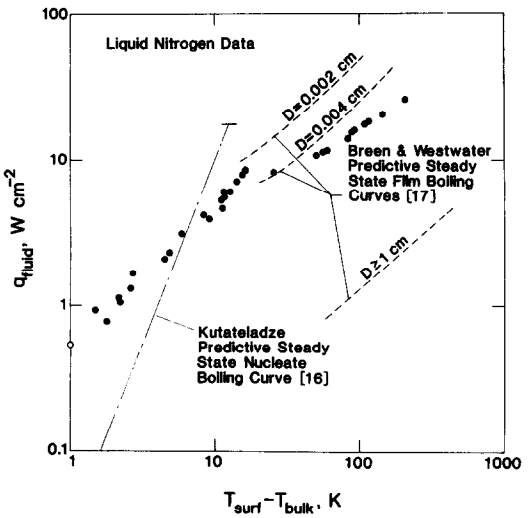

FIG. 7. Steady-state boiling heat transfer data for small diameter wire heater surface.

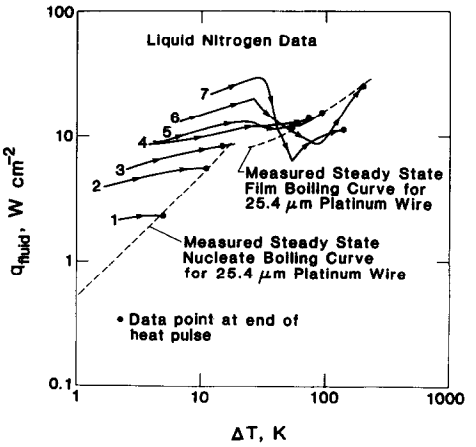

FIG. 8(a). Transient boiling heat transfer data for small diameter wire heater surface: Curve 1, 2.2 W cm^{-2} at t_0, time period, 0.001–10 s; Curve 2, 5 W cm^{-2} at t_0, time period, 0.001–10 s; Curve 3, 7.5 W cm^{-2} at t_0, time period, 0.001–10 s; Curve 4, 10 W cm^{-2} at t_0, time period, 0.001–1 s; Curve 5, 12 W cm^{-2} at t_0, time period, 0.001–1 s; Curve 6, 18 W cm^{-2} at t_0, time period, 0.001–0.1 s; Curve 7, 33 W cm^{-2} at t_0, time period, 0.001–0.01 s.

surface temperature began to decrease. Oker and Merte cited the analysis of Goldstein and Briggs [15] which predicts that the onset of natural convection from a vertical surface is inversely proportional to the 2/5 power of the heat flux. The data of this study and others follow the trend of Oker and Merte's data and indicated a much stronger influence of heat flux (approximately proportional to $1/q^2$, see the appendix).

Although not a clear-cut distinction, it appears that for a given heat flux, the wire geometry time to onset of convection is about twice that of the flat surface geometry.

Traditionally, boiling heat transfer data are presented in the form of heat flux vs surface temperature rise, as shown in Figs. 7–9 for both steady-state and transient data. Figure 7 contains the steady-state data for the horizontal wire geometry. Whereas the classical nucleate boiling correlation shown [16] predicts heat flux proportional to about the 2.5 power of ΔT, the experimental heat flux is approximately linear with ΔT. The experimental film boiling data also indicate a less pronounced variation of heat flux with ΔT when compared with the predictive correlation of Breen and Westwater [17]. Finally, the steady-state experimental peak nucleate boiling heat flux (approximately 8.5 W cm^{-2}) is about half of that predicted by the Kutateladze correlation. This may be due to the small size of the wire which may be more readily blanketed by coalescing bubbles. Sinha [14] reported that transient heating of a vertical platinum wire produces a premature transfer to film boiling at heat fluxes as low as 40% of the steady-state critical heat flux. No premature transition to film boiling was observed for the horizontal platinum wire of this study. No attempt was made to maintain a highly quiescent liquid bath, and this may account for the absence of a premature film boiling transition since Sinha reported a decided effect of convection on the level of the transition heat flux.

Figure 8(a) presents transient q vs ΔT, for the wire geometry. Each curve corresponds to a different applied heat flux at time zero and for a duration noted in the legend for the graph. Results are shown in Fig. 9 for the thin platinum film heater surface. One may

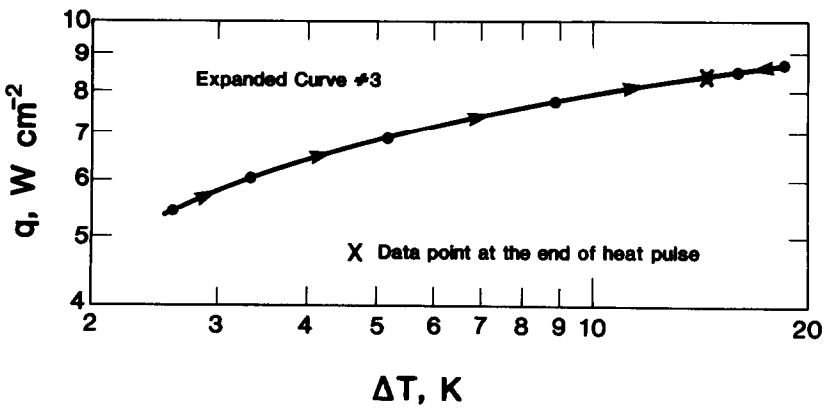

FIG. 8(b). Illustration of small temperature 'overshoot' for platinum wire [Curve 3, Fig. 8(a)].

observe some striking differences between these two figures. First, there is very little ΔT 'overshoot' before the onset of nucleate boiling in the case of the platinum wire. The small overshoot can be seen in Fig. 8(b) where Curve 3 of Fig. 8(a) is plotted on an expanded scale. However, the thin film surface produces a substantial overshoot as seen by the reversal of the arrows on the curves in Fig. 9. This 'overshoot' may also be seen, for example, in Fig. 3, Curves 7.5 and 2.8 W cm^{-2}, where the ΔT rises momentarily to a value above the steady-state value.

The steady-state data for the thin film surface, Fig. 9, are limited and thus the peak nucleate boiling heat flux and the nucleate boiling curve were not well established. However, the peak is estimated to be about 8.5 W cm^{-2} since Curve 5 is considered to be very near the peak nucleate boiling heat flux at 20 K. The experimental peak nucleate boiling heat flux is, as for the wire, about half of that predicted by Kutateladze. The thermal properties of the quartz substrate, $\sqrt{(\rho C_p k)}$, are presumed to account for this reduced value since several investigations, e.g. Grigoriev *et al.* [18], have found that the peak nucleate boiling heat flux is proportional to $\sqrt{(\rho C_p k)}$ of the heater surface (see Fig. A1 in the appendix). Since the heater surface in this study is a very thin platinum film (35 nm) the thermal properties of the quartz substrate dominate. For the limited data, it appears that the experimental steady-state nucleate boiling curve has a slope in fair agreement with the predicted curve, in contrast to the slope for the wire geometry. Due to concern for 'burning out' the thin film sample, steady-state film boiling data was not attained for the flat surface. However, as can be seen, the trend of Curves 5 and 6 is toward the Breen and Westwater steady-state film boiling correlation. From Fig. 8(a) one may note that the short duration transient heat transfer may be significantly higher than the corresponding steady-state heat transfer at the same ΔT. This is the trend for the nucleate boiling regime, however, and for the film boiling regime the opposite may be true.

For the thin film geometry, Fig. 9, the pronounced hysteresis during the transient makes it difficult to generalize with regard to improved or degraded heat transfer as compared to the steady-state heat transfer.

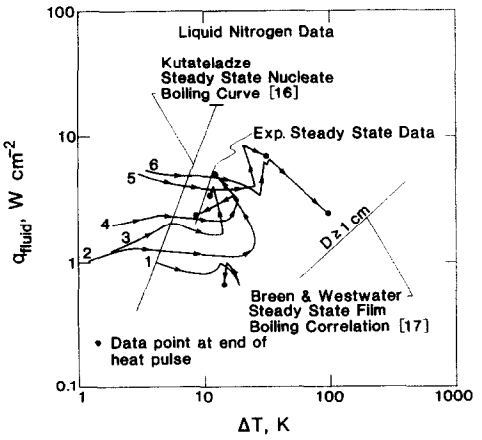

FIG. 9. Transient boiling heat transfer data for vertical platinum film heater surface: Curve 1, 1.68 W cm^{-2} at t_0, time period, 0.002–10 s; Curve 2, 2.8 W cm^{-2} at t_0, time period, 0.001–10 s; Curve 3, 4.2 W cm^{-2} at t_0, time period, 0.001–10 s; Curve 4, 5.3 W cm^{-2} at t_0, time period, 0.001–10 s; Curve 5, 9.2 W cm^{-2} at t_0, time period, 0.001–1 s; Curve 6, 10.2 W cm^{-2} at t_0, time period, 0.001–1 s.

SUMMARY

(1) The heat transfer coefficient during the early part of a transient heat pulse may be predicted by classical transient pure conduction equations.

(2) The time to onset of convection is proportional to approximately $1/q^2$.

(3) The steady-state nucleate boiling heat flux varies linearly with ΔT for the wire geometry and varies approximately as $\Delta T^{2.5}$ for the thin film flat surface geometry.

(4) The experimental steady-state peak nucleate boiling heat flux is about half that predicted by classical correlations but for these data there is no evidence of a premature transition to film boiling under transient heating conditions.

(5) For the wire geometry, the short duration heat transfer may be higher than the corresponding steady-state value at the same ΔT, however, for the thin film flat surface on a quartz substrate, hysteresis effects make it difficult to make a similar generalization.

REFERENCES

1. W. G. Steward, Transient helium heat transfer phase I – static coolant, *Int. J. Heat Mass Transfer* **21**, 863–874 (1978).
2. P. J. Giarratano and N. V. Frederick, Transient pool boiling of liquid helium using a temperature controlled heater surface, *Adv. Cryogen. Engng*, Vol. 25, pp. 455–466. Plenum Press, New York (1980).
3. P. J. Giarratano and W. G. Steward, Transient forced convection heat transfer to helium during a step in heat flux, *Trans. Am. Soc. Mech. Engrs* **105**, 350–357 (1983).
4. H. Kawamura, Experimental and analytical study of transient heat transfer for turbulent flow in a circular tube, *Int. J. Heat Mass Transfer* **20**, 443–450 (1977).
5. P. J. Giarratano, F. L. Lloyd, L. O. Mullen and G. B. Chen, A thin platinum film for transient heat transfer studies, *6th Int. Temp. Symp.*, Vol. 5, pp. 859–863 (1982).
6. H. M. Roder, A transient hot wire thermal conductivity apparatus for fluids, *J. Res. Natn. Bur. Stand.* **86**(5), 457–493 (1981).
7. C. D. Hodgman, R. C. Wast, R. S. Shankland and M. S. Selby, *Handbook of Chemistry and Physics* (43rd edn.). Chemical Rubber Publ. Co., Cleveland, Ohio (1962).
8. Y. S. Touloukian and E. H. Buyco, *Thermophysical Properties of Matter*, Vol. 4, pp. 165–166 (Curves 5 and 6). IFI/Plenum, New York (1970).
9. N. K. Madsen and R. F. Sincovec, Algorith 540 PDECOL, general collocation software for partial differential equations [D3], *ACM Trans. Math. Software* **5**(3), 326–351 (1979).
10. Y. S. Touloukian, R. W. Powell, C. Y. Ho and P. G. Klemens, *Thermophysical Properties of Matter*, Vol. 2, p. 193. IFI/Plenum, New York (1970).

11. H. S. Carslaw and J. C. Jaeger, *Conduction of Heat in Solids* (2nd edn.). Oxford University Press, Oxford (1948).
12. E. Oker and H. Merte, Jr., *6th Int. Heat Transfer Conf.*, Part I, pp. 139–144. Hemisphere, Washington, DC (1978).
13. O. Tsukamoto, T. Uyemura and T. Uyemura, Observation of bubble formation mechanism of liquid nitrogen subjected to transient heating, *Adv. Cryogen. Engng*, Vol. 25, pp. 476–482. Plenum Press, New York (1980).
14. D. N. Sinha, Studies of homogeneous nucleation and transient heat transfer in cryogenic liquids, Ph.D. thesis, Portland State University (1980).
15. R. J. Goldstein and D. G. Briggs, *Trans. Am. Soc. Mech. Engrs*, Series C, *J. Heat Transfer* **86**, (1964).
16. S. S. Kutateladze, Heat transfer in condensation and boiling, State Sci. and Tech. Publ. of Lit. on Machinery, Moscow, AEC Translation 3770, Tech. Info. Service, Oak Ridge, Tennessee (1949, 1952).
17. B. P. Breen and J. W. Westwater, Effect of diameter of horizontal tubes on film boiling heat transfer, *Chem. Engng Prog.* **58**, 67–72 (1962).
18. V. A. Grigoriev, V. V. Klimenko, Yu. M. Pavlov and Ye. V. Ametistov, The influence of some heating surface properties on the critical heat flux in cryogenic liquids boiling, *6th Int. Heat Transfer Conf.*, Vol. 1, p. 215 (1978).
19. Lord Rayleigh, On convection currents in a horizontal layer of fluid when the higher temperature is on the under side, *Phil. Mag.* **32**, 529 (1916).
20. H. Gröber, S. Erk and U. Grigull, *Fundamentals of Heat Transfer*, p. 315. McGraw-Hill, New York (1961).

APPENDIX

Dependence of 'time to onset of convection' on $1/q^2$

For a horizontal layer heated from below, Lord Rayleigh [19] noted that at a critical value of *Gr Pr* (referred to as the Rayleigh number, *Ra*) the unstable stratification in the fluid would break down resulting in convective motion. Similar observations of Ra_{crit} have been made for vertical heated layers and are reported in ref. [20]. The critical Rayleigh number concept is used to support the $1/q^2$ dependence of τ exhibited by our data.

$$Ra_{crit} = (Gr\ Pr)_{crit} = C_1, \tag{A1}$$

now

$$Gr_{crit} = \frac{g\beta\Delta T L^3}{\nu^2}, \tag{A2}$$

where g is the gravitational constant, $\beta = 1/V(\mathrm{d}V/\mathrm{d}t)$ is the compressibility, $\nu = \mu/\rho$, is the kinematic viscosity, $\Delta T = T_{surf} - T_{bulk}$, is the temperature difference, and L is the heater length. For pure conduction in the fluid, which is the mechanism of heat transfer up to the onset of convection

$$\Delta T = \frac{2q_0}{k}\left(\frac{\alpha\tau}{\pi}\right)^{1/2}. \tag{A3}$$

(This is equation (7) in the text.) Substituting equation (A3) in equation (A2) results in

$$Gr_{crit} = \frac{g\beta C_2 q_0 \tau^{1/2} L^3}{\nu^2},$$

where

$$C_2 = \frac{2}{k}\left(\frac{\alpha}{\pi}\right)^{1/2}.$$

Solving for $\tau^{1/2}$ and squaring the result

$$\tau_{crit} = \frac{Gr_{crit}^2 \nu^4}{g^2\beta^2 C_2^2 q_0^2 L^6}, \tag{A4}$$

which shows

$$\tau_{crit} \propto \frac{1}{q_0^2}.$$

Experimental error

Experimental uncertainty in the heat transfer coefficient is determined primarily by the heat pulse duration and magnitude, at least for short times. The minimum usable pulse is that for which the temperature rise is comparable with the digitizing noise in the temperature measurements (originating in the digital recording oscilloscope). The noise corresponds to about 0.3 K for the thin film and about 0.7 K for the platinum wire. The lower limit of energy $(q\Delta t)_{min}$ for the thin film is about 0.0002 J cm^{-2} and for the platinum wire 0.002 J cm^{-2}. At these limits, the experimental uncertainty would be approximately 100%. For longer or larger pulses, the experimental error resulting from temperature measurement uncertainty is reduced, and other error sources become important, primarily the substrate correction for the thin films. Under the best experimental conditions the error in h_{exp} is as low as $\pm 5\%$.

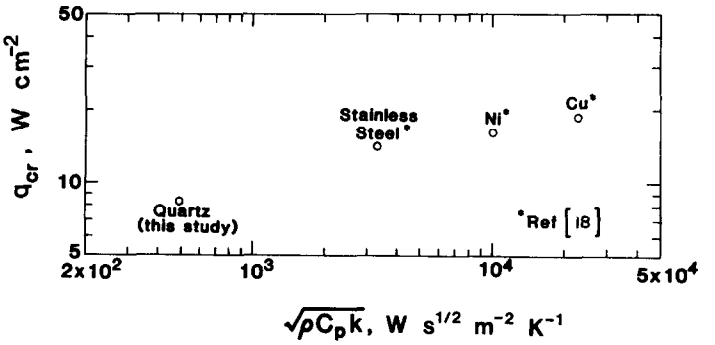

FIG. A1. The effect of thermal properties of heater surfaces on the peak nucleate boiling heat flux, q_{cr}.

TRANSFERT THERMIQUE VARIABLE PAR EBULLITION POUR DEUX DIFFERENTES SOURCES DE CHALEUR: FIL FIN ET COUCHE FINE SUR UN SUBSTRAT EN QUARTZ

Résumé—Des expériences sur le transfert thermique variable par ébullition sont décrites pour deux géométries différentes de surface chauffante submergée dans l'azote liquide. Pendant la première partie de la poussée thermique transitoire, le coefficient de transfert thermique pour les deux géométries s'accorde généralement avec les prévisions à partir des équations classiques de la conduction pure variable. L'accord persiste jusqu'à l'instant de la mise en place de la convection qui varie approximativement comme $1/q^2$ où q est le flux de chaleur transféré au fluide.

DER WÄRMEÜBERGANG BEIM INSTATIONÄREN SIEDEN AN ZWEI VERSCHIEDENEN WÄRMEQUELLEN: EIN DRAHT MIT KLEINEM DURCHMESSER UND EIN EBENER, DÜNNER FILM AUF EINER QUARZUNTERLAGE

Zusammenfassung—Es werden Wärmeübergangsdaten an zwei Heizoberflächen verschiedener Geometrie, welche in flüssigen Stickstoff eingetaucht sind, mitgeteilt. In der Anfangsphase des instationären Wärme-Impulses stimmt der Wärmeübergangskoeffizient im allgemeinen für beide Geometrien mit den Werten überein, die mit klassischen Gleichungen für reine instationäre Wärmeleitung erhalten werden. Die Übereinstimmung besteht bis zum Zeitpunkt des Einsetzens der Konvektion, welcher sich etwa aus $1/q^2$ ergibt, wobei q die Wärmestromdichte an das Fluid ist.

ТЕПЛОПЕРЕНОС ПРИ НЕСТАЦИОНАРНОМ КИПЕНИИ ОТ ДВУХ РАЗЛИЧНЫХ ИСТОЧНИКОВ ТЕПЛА: ПРОВОЛОКИ МАЛОГО ДИАМЕТРА И ПЛОСКОЙ ПОВЕРХНОСТИ ТОНКОЙ ПЛЕНКИ НА КВАРЦЕВОЙ ПОДЛОЖКЕ

Аннотация—Приведены данные по теплопереносу при нестационарном кипении для двух различных геометрий поверхности нагревателя, погруженного в жидкий азот. В обоих случаях коэффициент теплообмена для начальной стадии переходного режима в общем согласуется со значениями, рассчитанными по классическим уравнениям чистой нестационарной теплопроводности. Согласие сохраняется вплоть до времени возникновения конвекции, которое изменяется примерно как $1/q^2$, где q—тепловой поток к жидкости.